

Investigations into the Biosynthesis of Porphyrins and Corrins— Calculations on 1,3-Allylic Strain and [1,5]-Sigmatropic Rearrangements in Pyrroles, Furans, and Thiophenes

Lutz F. Tietze* and Gerhard Schulz

Dedicated to Professor Hans Paulsen on the occasion of his 75th birthday

Abstract: The [1,5]-sigmatropic rearrangements of hydrogen and other groups, such as methyl, *tert*-butyl, allyl, benzyl, and azafulvenium, in pyrroles and, to some extent, in furans and thiophenes, has been studied by using semiempirical and ab initio methods. These systems are used as models to explain the ring D inversion in the biosynthesis of uroporphyrinogen III and the stereoselec-

tive shift of a methyl group in the biosynthesis of vitamin B₁₂. The difference in energy between the competing pathways of hydrogen and methyl shifts is signifi-

cantly lower than for cyclopentadiene. The rearrangements are usually concerted, except for in strongly resonance-stabilized systems, such as azafulvenium cations. Furthermore, ab initio calculations of the 1,3-allylic strain for a range of substituted pyrroles has been performed, and the results compared with semiempirical data.

Keywords

ab initio calculations • biosynthesis • porphyrinogens • rearrangements • semiempirical calculations

Introduction

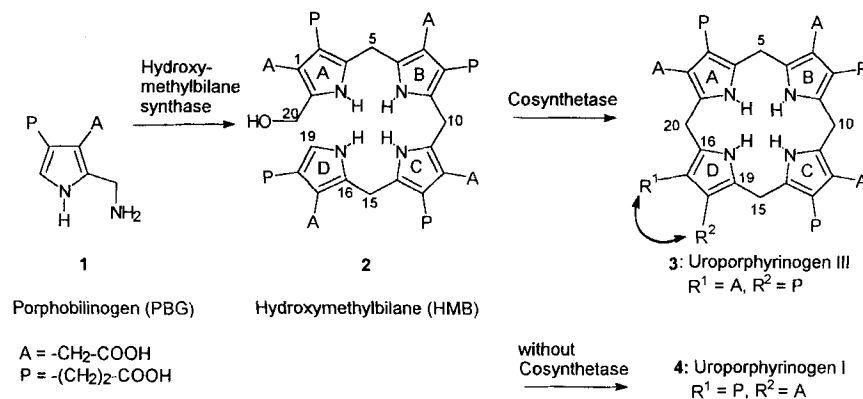
The cyclic tetrapyrrole uroporphyrinogen III (**3**) is the biosynthetic precursor for chlorophylls, bacteriochlorophylls, heme, siroheme, coenzyme F430, and vitamin B₁₂, which are known as the pigments of life.^[1] Uroporphyrinogen III is formed from porphobilinogen (PBG, **1**) via hydroxymethylbilane (HMB, **2**) by the action of the enzymes hydroxymethylbilane synthase (HMBS) and uroporphyrinogen III synthase (cosynthetase); HMB (**2**) was shown to be a non-enzyme-bound intermediate.^[2]

A remarkable step in the biosynthesis of uroporphyrinogen III (**3**) is the inversion of ring D, which takes place only in the presence of cosynthetase.^[3] In the absence of this enzyme only physiologically inactive uroporphyrinogen I (**4**) is formed, which does not isomerize to give **3** even when treated with cosynthetase.^[3b]

Several mechanisms for the formation of uroporphyrinogen III (**3**) have been proposed in the past; however, none of these have been verified, and none have been able to explain the high selectivity of the rearrangement. We recently introduced a

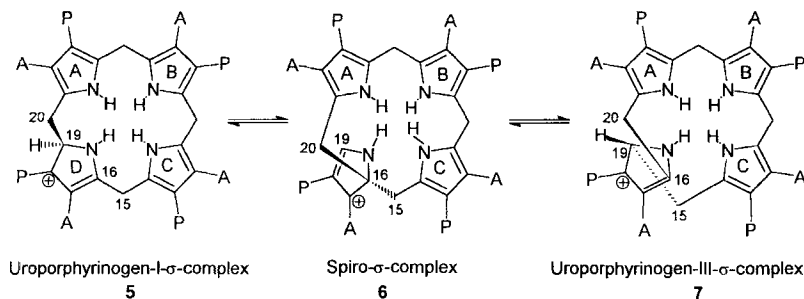
new mechanism for the inversion of ring D based on semiempirical calculations of the conformational preference of tetrapyrroles^[4] and of the transition-state structure for the cyclization.^[5] According to experimental work^[4] and our calculations, we proposed that, through the action of the enzyme cosynthetase, hydroxymethylbilane (**2**) is first stereoselectively transformed into the chiral uroporphyrinogen I σ complex **5** (or its enantiomer) in a kinetically controlled reaction (Scheme 2); in this process the hydroxyl group in **2** is protonated by an acid moiety in the enzyme and dehydrated. Then, in an equilibrium, **5** can give the uroporphyrinogen III σ complex **7** (or its enantiomer).

The might involve several suprafacial [1,5]-sigmatropic rearrangements or a sterically controlled two-step mechanism, presumably via the spiro σ complex **6**, which is, however, much higher in energy than **5** and **7**. The uroporphyrinogen III σ



Scheme 1. Biosynthesis of uroporphyrinogen III.

[*] Prof. Dr. Dr. h. c. L. F. Tietze, Dr. G. Schulz
Institut für Organische Chemie der Georg-August-Universität Göttingen
Tammannstraße 2, D-37077 Göttingen (Germany)
Fax: Int. code +(551)39-9476



Scheme 2. Proposed mechanism for the formation of uroporphyrinogen III (3).

complex **7** finally collapses to give uroporphyrinogen III (**3**). The enzyme cosynthetase prevents the direct abstraction of a proton from uroporphyrinogen I σ complex **5** to give uroporphyrinogen I (**4**). Its mode of action can be explained in terms of the fixation of HMB (**2**) into a cyclic conformation and the kinetic stabilization of **5**, owing to the lack of a base appropriately positioned in the enzyme pocket for the deprotonation of **5**.

Clearly, the activation energy for the elimination of a proton from the uroporphyrinogen I σ complex **5** must be higher than for the rearrangement to give the uroporphyrinogen III σ complex **7**. We further proposed that the elimination of a proton from **7** is fast compared to that from **5**, because the hydrogen in **7** has the opposite steric orientation to that in **5**; the anion of the acid moiety in the enzyme is now favorably oriented to act as a base and can abstract the hydrogen to give uroporphyrinogen III (**3**). In the course of this process the active species of the enzyme is restored.

In this paper we present calculations on the mechanism of the rearrangement of the uroporphyrinogen I σ complex **5** to give the uroporphyrinogen III σ complex **7**. For the proposed mechanism it is important to know whether an alkyl shift in pyrroles is concerted or stepwise and how electronic and steric factors influence the reaction. In addition we investigate whether substituted pyrroles exhibit an allylic 1,3-strain.

Computational Procedure

Ab initio calculations were performed with the program package GAUSSIAN 92^[6] of the Zentralinstitut für Angewandte Mathematik (ZAM), Kernforschungsanlage (KFA) Jülich. For calculations of 1,3-allylic strain the geometries were partially optimized as a function of the dihedral angle $\angle \text{H}_a - \text{C}_b - \text{C}_c = \text{C}_d$ with the values of 0, 60, 90, 100, 110, 120, 170, and 180° by using the RHF/3-21G basis set;^[7] all other variables were optimized by a MP2/6-31G*//RHF/3-21G single-point calculation.^[8,9]

The semiempirical results were obtained by an increase in the torsional angle in steps of 10° between 0 and 180° and partial optimization with the VAMP^[10] or MOPAC 6.0^[11] package for both AM1^[12] and PM3^[13] Hamiltonians.

For the calculations of transition-state structures the standard split-valence RHF/3-21G basis set was used for pre-optimization in conjunction with full TS optimization of all variables, following the same procedure as described above, using the RHF/6-31 + G* basis set and single-point calculations at the MP2/6-31G*//RHF/6-31G* level; the results of the lower level calculations are presented in ref. [14]. The authenticity of the transition-state structures was ensured by vibrational frequency calculations. Semiempirical transition-state structures were calculated with the RHF/AM1 or PM3 method using the NS01A^[15] subroutine followed by normal vibration analysis with a FORCE calculation.

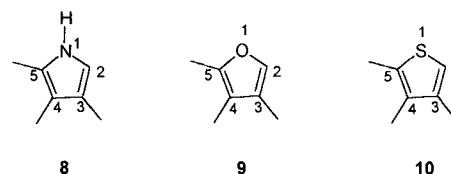
All energies in this text are given in kcal mol⁻¹, and bond lengths in Å. Unless stated otherwise, the discussion of ab initio results is based on the geometries obtained with the RHF/6-31 + G*//RHF/6-31 + G* basis set and on the energies obtained with MP2/6-31 + G*//RHF/6-31 + G* basis set.

Results and Discussion

Ab initio studies on the methyl and hydrogen shifts

in heteroarenes: As mentioned in the Introduction, we propose two possible mechanisms for the enzymatic transformation of hydroxymethylbilane (**2**) into uroporphyrinogen III (**3**), involving suprafacial [1,5]-sigmatropic rearrangements or stepwise sterically controlled migrations of the substituents at C2 and C5. So far, no calculations have been performed on sigmatropic rearrangements of heterocycles such as pyrroles, furans, and thiophenes. The only data available on this type of rearrangement is for cyclopentadienes.^[16]

For our calculations we employed 3,4,5-trimethylpyrrole (**8**), 3,4,5-trimethylfuran (**9**), and 3,4,5-trimethylthiophene (**10**) as



model systems (for numbering, see ref. [17]). Besides their specific relevance to the biosynthesis of uroporphyrinogen III (**3**), these systems are also of general interest since furans and thiophenes are often found in porphyrin homologues and porphyrinoids.^[18] In addition, [1,5]-sigmatropic methyl shifts in pyrrole systems are proposed to be involved in the biosynthesis of vitamin B₁₂ (e.g. precorrin-8 \times \rightarrow hydrogenobyric acid).^[19] Furthermore the results of the ab initio calculations are used to validate semiempirical calculations for the analysis of more complex systems that may be of synthetic interest.

The calculations (Tables 1a–3a) reveal that the lowest-energy cationic intermediates of **8–10** are substituted at C2^[17] (Figure 1). This can be explained by the number of resonance structures, which is greatest for the substrate with the cationic center at C3 and decreases for C2⁺ and again for X1⁺.

The stability of the cationic intermediates are highest for the pyrrole system **8**, followed by furan **9** and thiophene **10**. This is in agreement with experimental results.^[20] Of the three path-

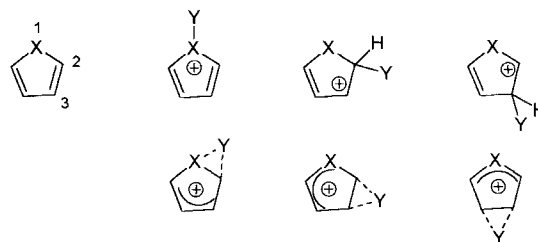
Figure 1. Possible intermediates and transition-state structures for hydrogen and methyl (Y = H, CH₃) shifts in pyrrole, furan, and thiophene (X = NH, O, S).

Table 1. Pyrrole system **8**.

a) Energies of intermediates protonated and methylated at the positions indicated (Figure 1, top).

	$E_{\text{rel}}(Y = \text{H})$ [a]	$E_{\text{rel}}(Y = \text{CH}_3)$ [a]
N1	19.81	21.46
C2	0.00	0.00
C3	5.40	7.77

b) Energies and geometries for the transition states (Figure 1, bottom) of the [1,5]-sigmatropic rearrangement of hydrogen and methyl (MP2/6-31+G**/RHF/6-31+G*).

A–B shift	A–H [b]	B–H [b]	E_{rel} [a]	A–C [b]	B–C [b]	E_{rel} [a]
N1–C2	1.250	1.327	49.08	2.115	2.231	60.07
C2–C3	1.314	1.326	25.11	1.923	1.959	31.49
C3–C4	1.300	1.300	25.70	2.032	2.032	39.49

[a] Relative energy [kcal mol⁻¹] referring to the lowest energy species (substitution at C2) without inclusion of zero-point energy (ZPE). [b] Bond length in Å.Table 2. Furan system **9**.

a) Energies of intermediates protonated and methylated at the positions indicated (Figure 1, top).

	$E_{\text{rel}}(Y = \text{H})$ [a]	$E_{\text{rel}}(Y = \text{CH}_3)$ [a]
O1	32.37	34.42
C2	0.00	0.00
C3	12.71	16.84

b) Energies and geometries for the transition states (Figure 1, bottom) of the [1,5]-sigmatropic rearrangement of hydrogen and methyl (MP2/6-31+G**/RHF/6-31+G*).

A–B shift	A–H [b]	B–H [b]	E_{rel} [a]	A–C [b]	B–C [b]	E_{rel} [a]
O1–C2	1.183	1.351	57.05	2.204	2.435	67.46
C2–C3	1.328	1.316	27.12	1.909	1.933	30.05
C3–C4	1.230	1.230	32.45	2.145	2.145	49.10

[a] Relative energy [kcal mol⁻¹] referring to the lowest energy species (substitution at C2) without inclusion of zero-point energy (ZPE). [b] Bond length in Å.Table 3. Thiophene system **10**.

a) Energies of intermediates protonated and methylated at the positions indicated (Figure 1, top).

	$E_{\text{rel}}(Y = \text{H})$ [a]	$E_{\text{rel}}(Y = \text{CH}_3)$ [a]
S1	26.60	15.40
C2	0.00	0.00
C3	8.72	16.40

b) Energies and geometries for the transition states (Figure 1, bottom) of the [1,5]-sigmatropic rearrangement of hydrogen and methyl (MP2/6-31+G**/RHF/6-31+G*).

A–B shift	A–H [b]	B–H [b]	E_{rel} [a]	A–C [b]	B–C [b]	E_{rel} [a]
S1–C2	1.476	1.469	40.09	–	–	–
C2–C3	1.354	1.281	24.41	1.950	1.914	28.26
C3–C4	1.301	1.301	25.92	2.095	2.095	37.75

[a] Relative energy [kcal mol⁻¹] referring to the lowest energy species (substitution at C2) without inclusion of zero-point energy (ZPE). [b] Bond length in Å.

ways for rearrangement of these heteroaromatic systems—shift from C2 to X1, C2 to C3, and C3 to C4—the rearrangement from C2 to C3 is the lowest in energy followed by the rearrangements from C3 to C4 and then from C2 to X1; the latter is much higher in energy and can therefore be neglected (Figure 1, Table 1b–3b). The energy differences between the pathways are lowest for the pyrrole **8**, followed by thiophene **10** and furan **9**.

Interestingly, the geometries of the TS for the rearrangements from C2 to C3 are quite similar for **8**–**10**. For the other hydrogen and methyl shifts in **8**–**10** the TS geometries differ significantly. For example, the C–H bond in the TS for the H shift from C3 to C4 in the furan system **9** is calculated to be shorter than that in the corresponding the pyrrole system **8**. In contrast, the calculated C–CH₃ bond in the methyl shift from C3 to C4 is longer for **9** than for **8**. The TS geometry of the thiophene system **10** is similar to that of the pyrrole **8**.

The difference in energy is usually more pronounced for the methyl shift than for the hydrogen shift. However, the situation differs from system to system. Compared to the pyrrole system, the hydrogen shift from C2 to C3 in furan is higher in energy, whereas the methyl shift from C2 to C3 is lower in energy. The methyl shift from C3 to C4 in furan is significantly higher in energy than for the pyrrole system. This may be explained by the different energies of the molecular orbitals involved (C3–C4 shift/AM1: pyrrole: –9.45 eV; furan: –10.64 eV; thiophene: –9.55 eV. C2–C3 shift/AM1: pyrrole: –8.66 eV; furan: –9.32 eV; thiophene: –9.22 eV). For the pyrrole system the lowest energy methyl shift is calculated to be only 6.38 kcal mol⁻¹ higher in energy than the lowest hydrogen shift; the difference found for the furan system is less than 3 kcal mol⁻¹. This strongly differs from the rearrangement of the cyclopentadiene systems, where the methyl shift is estimated to be 32 kcal mol⁻¹ higher in energy than the hydrogen shift.^[8]

It should be noted that the ab initio calculations are highly dependent on the basis set; with a few exceptions, the energies of activation estimated with the 6-31+G* basis set are higher than those calculated by using 3-21 G.^[21]

Semiempirical calculations on the hydrogen and methyl shifts in the pyrrole system:

The energies and geometries obtained for the hydrogen and methyl shifts in the pyrrole system by ab initio calculations will now be compared with semiempirical data. AM1 estimates the bonds to be too long for the methyl shift, whereas PM3 gives nearly identical geometries to the ab initio method (RHF/6-31+G* optimized geometry). For the hydrogen shift both AM1 and PM3 overestimate the bond lengths relative to the ab initio results (Tables 1 and 4). In addition PM3

Table 4. Semiempirical calculations of the energies (kcal mol⁻¹) and geometries (Å) for the transition states of the [1,5]-sigmatropic rearrangement of hydrogen and methyl in the pyrrole system **8**.

	A–B shift	A–H	B–H	E_{rel}	A–C	B–C	E_{rel}
AM1	N1–C2	1.34	1.42	55.09	2.15	2.28	72.93
	C2–C3	1.41	1.43	33.42	2.10	2.12	45.83
	C3–C4	1.41	1.41	33.64	2.14	2.14	49.73
PM3	N1–C2	1.42	1.48	53.02	1.95	2.03	65.00
	C2–C3	1.44	1.45	31.46	2.01	2.02	45.03
	C3–C4	1.44	1.44	30.06	2.03	2.03	46.33

estimates the hydrogen migration from C3 to C4 to be energetically more favorable than that from C2 to C3, in disagreement with the ab initio calculations; therefore, PM3 should not be used for a theoretical description of [1,5]-sigmatropic rearrangements in pyrroles.

Both semiempirical methods estimate the substrate protonated at C3 to be lowest in energy,^[14] again disagreeing with the ab initio method. The energies of activation are more or less correct for both methods; however, they are better reproduced by AM1. Although PM3 describes the geometrical aspects better than AM1, AM1 is in better agreement with the relative energies of the ab initio results, and we therefore chose the latter for the semiempirical studies.

The MO coefficients (Figure 2) favor an electrophilic attack at C2 and C5; however, C2^[17] is sterically less hindered. The

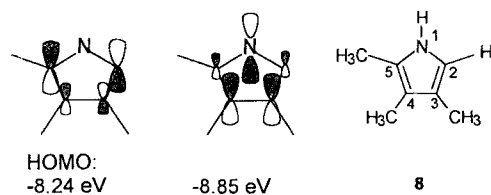


Figure 2. Electronic structure of the pyrrole **8**.

shift from C2 to C3 is directed by the HOMO; the shift from C3 to C4 is controlled by an MO that is approximately 0.6 eV more negative in energy, and thus proceeds with a significantly higher energy of activation. In this AM1/RHF study no TS is found for an electrophilic attack of a cation E⁺ at **8**, but the TS geometries are identical with those of the [1,5]-sigmatropic rearrangement. This three-center TS therefore provides the best possible stabilization for the charge of the cation. The TS for the sigmatropic [1,5]-methyl shift in **8** exhibits slightly longer bond lengths than pyrrole; this can be traced back to steric interactions with the substituents. In this way it can be explained why the intermediate substituted at C2 (analogous to uroporphyrinogen I or III σ complexes **5** or **7**) is lower in energy by 8.6 kcal mol⁻¹ than the intermediate methylated at C5 (analogous to the spiro σ complex **6**), in agreement with previous results.^[5] As already mentioned the sigmatropic hydrogen transfer is 6.38 kcal mol⁻¹ lower in energy than the lowest-energy path of the [1,5]-methyl shift. However, this lower energy of activation does not conflict with our model, since the hydrogen shift occurs suprafacially with retention of configuration and the products are kinetically stabilized owing to the lack of an appropriately oriented base in the enzyme pocket to abstract a hydrogen. On the other hand, in the biosynthesis of uroporphyrinogen III (**3**) it is a highly resonance-stabilized pyrrole-methyl group that migrates. We therefore decided to investigate the shift of allyl, *tert*-butyl, benzyl, and azafulvenium cations in pyrrole; in addition the rearrangements of these groups in the sterically crowded pyrrole **11** was compared with the migrations in the cyclopentadienes **12a–d** and **13a–d**, in order to determine the relative importance of steric interactions and resonance stabilization (Table 5).

The calculations reveal that the activation energy for the shift of the allyl, *tert*-butyl, and benzyl group is lower than the

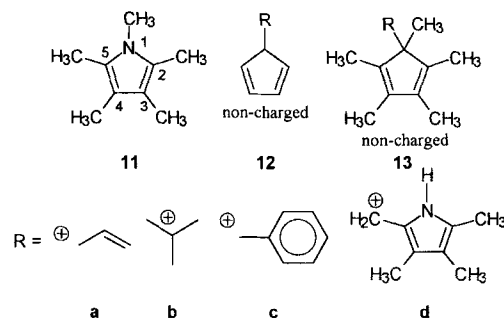


Table 5. Semiempirical structural and energetics data for the transition states of the [1,5]-sigmatropic rearrangements of different groups (a–d) in pyrrole, in the methylated pyrrole **11**, and in the neutral cyclopentadienes **12** and **13** (AM1/RHF).

Group	System	A–B shift	ΔH^\ddagger [kcal mol ⁻¹]	Δ -C ⁺ [Å]	B–C ⁺ [Å]	
allyl	pyrrole	1–2	51.58	2.45	3.11	
		2–3	36.88	2.27	2.28	
		3–4	38.93	2.32	2.33	
	11	1–2	71.73	2.44	3.09	
		2–3	57.20	2.28	2.29	
		3–4	59.91	2.33	2.34	
	12a			57.16	2.12	2.12
		13a			2.16	2.18
	<i>tert</i> -butyl	pyrrole	1–2			
2–3			38.61	2.43	2.50	
3–4			34.96	3.40	3.43	
11		1–2				
		2–3				
		3–4				
12b				56.34	2.20	2.21
		13b			2.27	2.28
benzyl		pyrrole	1–2	50.84	2.42	2.42
	2–3		36.58	2.32	2.36	
	3–4		37.62	2.42	2.42	
	11	1–2				
		2–3	52.95	2.34	2.38	
		3–4	54.84	2.45	2.45	
	12c			56.81	2.12	2.12
		13c			2.17	2.20
	azafulvenium	12d		55.34	2.15	2.14
13d			53.83	2.18	2.23	

ground-state energy found for the corresponding cations. In order to allow comparison of the data within this paper, the ΔH^\ddagger values given in the Tables refer to the positively charged pyrroles alkylated at C2. As expected for the sterically crowded pyrrole **11**, the energy of activation is significantly higher than for the parent system, that is, pyrrole itself; this result must be due to steric interaction. However, the bonds are only slightly lengthened in the TS of **11**; in some cases, such as for the azafulvenium cation, a TS could not be located. Since the latter is the model for the hydroxymethylbilane system, this particular reaction is examined in detail below. For the analogous migrations in cyclopentadienes a TS was located in all cases, of higher energy for the migration in the pyrrole. Interestingly, the energy of activation for the crowded cyclopentadienes **13a–d** is about 2 kcal mol⁻¹ lower than for **12a–d**, and the bond lengths are significantly lengthened. Thus, for the rearrangement in the cyclopentadienes charge stabilization and steric interactions are not determining in the TS, but rather charge separation.

In contrast, in the pyrrole systems there is a strong dependence on the stabilization of charge and on steric interactions.

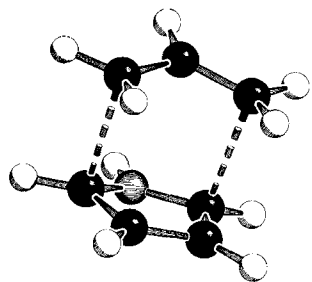


Figure 3. [4+3]-Sigmatropic rearrangement of the allyl cation at pyrrole as the lowest energy pathway (AM1/RHF).

Thus, the shift of the *tert*-butyl group has the highest energy of activation, allyl and benzyl rearrangements are similar in energy, and the shift of the azafulvenium group follows a different mechanism (see below). Interestingly, a new type of [4+3]-sigmatropic rearrangement was found for the shift of the allyl cation at pyrrole (Figure 3). This TS, containing a plane of symmetry and with C–C bond lengths of 2.32 Å, is on the lowest energy pathway in this system ($\Delta H^\ddagger = 34.30 \text{ kcal mol}^{-1}$). This pathway is favored owing to reduced steric interactions and charge distribution over seven atoms in the TS. Thus, the mechanism of the rearrangement at pyrroles and cyclopentadienes are quite different.

Hypersurfaces for the rearrangement of benzyl or azafulvenium cations in heteroarenes: In order to determine the details of the mechanism of rearrangement of benzyl and azafulvenium ions in the heteroarenes, the hypersurfaces for the reaction of these cations at C3 and C2 of the trimethylated pyrrole **8**, furan **9**, and thiophene **10** were determined by using AM1/RHF (Table 6).

Table 6. Semiempirical structural and energetics data for the transition state of [1,5]-sigmatropic rearrangement of the benzyl cation from C2 to C3 (a) and electrophilic attack of the azafulvenium ion at C2, C3, and C5 (b) in **8–10** (AM1/RHF).

a) Benzyl.

	ΔH^\ddagger [kcal mol ⁻¹]	C ⁺ –C2 [Å]	C ⁺ –C3 [Å]
8	30.05	2.56	2.35
9	38.27	2.35	2.29
10	39.55	2.48	2.11

b) Azafulvenium ion.

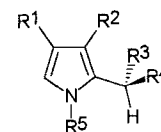
	Cx	ΔH^\ddagger [kcal mol ⁻¹]	C ⁺ –C2 [Å]	C ⁺ –Cx [Å]
8	C2	17.19	2.02	
	C3	22.18		2.03
	C5	21.10		2.11
9	C2	27.72	2.17	
	C3	31.41		2.05
10	C2	21.29	2.08	
	C3	31.41		1.93

These compounds exhibit the same substitution pattern as hydroxymethylbilane (**2**). The distances of the benzyl and of the azafulvenium cation to C2 and C3, respectively, were varied in steps of 0.1 Å.

The hypersurfaces for all systems are nearly identical. Thus, the three systems **8–10** exhibit similar reactions, as was already deduced from the results of the ab initio calculations. The point of lowest energy is always the intermediate with the migrating group at C2, which is the analogue for uroporphyrinogen I σ

complex **5**. However, there is an important difference between the hypersurfaces of the benzyl and the azafulvenium shift. For the benzyl system the energy of the isolated species is not a minimum, but increases with elongation of the C–C bonds; thus, the reaction should follow a concerted [1,5]-sigmatropic rearrangement, because a hypothetical intermediate consisting of separated species is higher in energy. In contrast, in the rearrangement of the azafulvenium ion the energy for the isolated species is a minimum; it follows that a two-step mechanism is operating with the electrophilic attacks at C2 and at C3 each having one TS. Moreover, it has to be assumed that the isolated cationic intermediates are further stabilized by entropic factors and solvation, owing to their higher charge density compared with the TS. Thus, considering the Gibbs enthalpy and the contribution of solvation, the rearrangement of azafulvenium ions is expected to follow a two-step mechanism and that of the benzyl cation is on the borderline between concerted and two-step mechanism.

1,3-Allylic strain in pyrroles: 1,3-Allylic strain^[22] undoubtedly plays an important role in the control of conformation. In this manner we have explained the difference in the acid-catalyzed reaction of unsubstituted and substituted hydroxymethylpyrroles **14a** and **14b**;^[4] thus, **14b** gives 80% of the correspond-



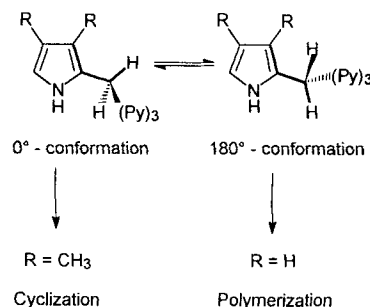
14

14	R ¹	R ²	R ³	R ⁴	R ⁵
14a	H	H	OH	H	H
14b	CH ₃	CH ₃	OH	H	H
14c	H	H	CH ₃	H	H
14d	H	H	CH ₃	CH ₃	H
14e	H	CH ₃	CH ₃	H	H
14f	H	CH ₃	CH ₃	CH ₃	H
14g	H	H	CH ₃	CH ₃	CH ₃

ing cyclic tetrapyrrole, whereas **14a** leads to a polymer. The AM1 calculations are in good agreement with this experiment (Scheme 3). However, to verify our assumption at a higher level we used ab initio methods.

The barriers of rotation for **14c–g** obtained by ab initio calculation agree quite well with the results of the AM1/RHF and PM3/RHF calculations.

The pyrroles that are expected to exhibit 1,3-allylic strain (**14e–g**) preferentially adopt a conformation in which the hydrogen of the substituent at C2 is synperiplanar to the substituent at C3 (Table 8). As expected, the systems **14c** and **14d** show a “normal” rotation curve (Table 7).^[8] The



Scheme 3. Different modes of reaction for substituted and unsubstituted tetrapyrroles influenced by 1,3-allylic strain (Py = methylene-pyrrole).

Table 7. Energies of rotation for **14c** and **14d** [kcal mol⁻¹].

		1st min	1st max [a]	2nd min [b]	2nd max [c]
14c	MP2/6-31 G*//3-21 G	0.00	1.43	-0.05	0.52
	MP2/6-31 G*//3-21 G [d]		0.49	0.27	
	AM1	0.00	0.11 (70°)	0.02	0.68
	AM1 [d]		0.74	0.70 (-110°)	
	PM3	0.00	0.69	-0.06 (130°)	0.19
	PM3 [d]	-0.05 (-20°)	0.67 (-120°)	-	-
14d	MP2/6-31 G*//3-21 G	0.00	1.47 (90°)	0.17	0.34
	AM1	0.00	1.13 (90°)	0.78	1.07 (150°)
	PM3	0.00	1.42 (90°)	0.28 (180°)	-

[a] At 60° unless otherwise stated. [b] At 120° unless otherwise stated. [c] At 180° unless otherwise stated. [d] Negative dihedral angles (see text).

Table 8. Energies of rotation for **14e-g** [kcal mol⁻¹].

		1st min	max [a]	2nd min [b]
14e	MP2/6-31 G*//3-21 G	0.00	1.04	-0.07 (120°)
	MP2/6-31 G*//3-21 G [c]		2.49	
	AM1	-0.03 (20°)	0.03 (70°)	-0.04 (100°)
	AM1 [c]		2.17	
	PM3	0.00	0.46	-0.51
	PM3 [c]	-0.57 (-60°)	2.17	
14f	MP2/6-31 G*//3-21 G	0.00	2.86 (100°)	0.92 (170°)
	AM1	0.00	2.54 (110°)	1.69 (170°)
	PM3	0.00	3.39 (110°)	-0.29
14g	MP2/6-31 G*//3-21 G	0.00	5.54 (110°)	1.37
	AM1	0.00	2.55 (110°)	0.16
	PM3	0.00	3.92 (120°)	-0.81

[a] At 90° unless otherwise stated. [b] At 180° unless otherwise stated. [c] Negative dihedral angles (see text).

AM1/RHF calculations are in significantly better agreement with the ab initio results than PM3/RHF calculations (the opposite is true for aliphatic systems^[23]). Thus, it is preferable to use the AM1 method rather than PM3 to reproduce 1,3-allylic strain in pyrroles. The barrier to rotation is higher for the *N*-methylated **14g** than for C3-methylated **14f**. This can be traced back to the fact that the aromatic C2-N bond in these compounds is shorter than the C2-C3 bond, and the steric interaction is therefore greater in **14g**. This result also supports the assumption that 1,3-allylic strain is based on steric interaction and has no electronic origin.^[23]

The rotation curve of **14e** is shown in Figure 4. The barrier in the left-hand section (negative dihedral angles) is a result of interactions of the rotating ethyl group with the substituent at C3 (i.e., 1,3-allylic strain). However, there is no stable conformation at -180° because the curve descends to a second minimum at +120°. The second barrier at +60° is due to interactions with the substituent at the nitrogen atom. Thus, the minima at 0 and 120° are enantiomeric conformations with the same energy.^[24] **14e** therefore exists in one principal conformation. The energy barrier at -120° estimated by AM1/RHF (2.2 kcal mol⁻¹) is in very good agreement with the ab initio results (MP2/6-31 G*//RHF/3-21 G: 2.49 kcal mol⁻¹). However, AM1 significantly underestimates the second barrier at +60° (0.06 kcal mol⁻¹ vs. 1.04 kcal mol⁻¹ for MP2/6-31 G*//RHF/3-21 G). For the non-methylated species **14c** the right-hand section is identical to that of **14e** in Figure 4, because interactions are similar in this region. However, the negative dihedral region exhibits a normal rotation curve with a low

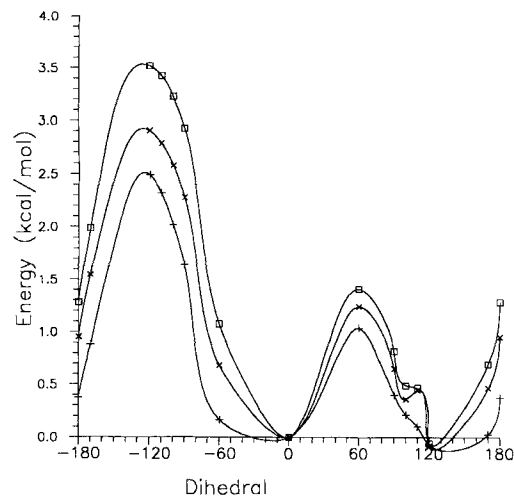


Figure 4. 1,3-Allylic strain - rotational barriers in **14e**: □: RHF/3-21 G; ×: RHF/6-31 G*//RHF/3-21 G; +: MP2/6-31 G*//RHF/3-21 G.

energy barrier at -60° and a minimum at -120°. In this case AM1 overestimates this second minimum (0.69 kcal mol⁻¹) relative to the ab initio results (MP2/6-31 G*//RHF/3-21 G: 0.27 kcal mol⁻¹). Thus, an even lower selectivity is to be expected for the reaction of **14c** than was predicted from the AM1 results.^[4]

Conclusion

The [1,5]-sigmatropic rearrangement in pyrrole, furan, thiophene, and cyclopentadiene systems was studied by semiempirical and ab initio methods in order to clarify similarities and differences in the mechanism. The results of AM1/RHF were shown to agree well with the ab initio findings for [1,5]-sigmatropic methyl shifts as well as for the description of 1,3-allylic strain in pyrroles. We found that the reaction pathways for hydrogen and methyl shifts differ by only 6.38 kcal mol⁻¹ for pyrrole (MP2/6-31 + G*//RHF/6-31 + G*) and less than 3 kcal mol⁻¹ for furan. Thus, in contrast to the situation in cyclopentadiene systems, methyl shifts compete successfully with hydrogen shifts. The energy of activation for the alkyl shift in heteroarenes is considerably reduced by charge stabilization. This is the case for the rearrangement of azafulvenium ions, which was shown to follow a two-step mechanism by analysis of the hypersurface. In contrast, the rearrangement of, for example, methyl or allyl cations is concerted. The [1,5]-sigmatropic alkyl shifts in heteroarenes such as pyrroles are also very sensitive to steric interactions; as an example, the [1,5]-shift of a *tert*-butyl group proceeds with a very high energy of activation. In contrast, the analogous migrations in cyclopentadienes have very similar activation energies.

The calculations yielded the following results for the biosynthesis of uroporphyrinogen III (**3**) from hydroxymethylbilane (**2**):

- 1) The kinetically controlled electrophilic attack of the hydroxymethyl group of ring A in hydroxymethylbilane (**2**) occurs at C19 in ring D to give the uroporphyrinogen I σ complex **5** and not at C16 to give the spiro compound **6**. This is consis-

- tent with the calculated difference in the activation energies for electrophilic substitution at C2 and C5 in **8** of $3.91 \text{ kcal mol}^{-1}$ in favor of attack at C2.^[17]
- The migration of the azafulvenium moiety in the uroporphyrinogen I σ complex **5** to give the uroporphyrinogen III σ complex **7** is thought to follow a sterically controlled two-step mechanism (cleavage and recombination) via the spiro σ complex **6** and not several suprafacial [1,5]-sigmatropic rearrangements. This is in agreement with the observation that ring D in hydroxymethylbilane is sterically fixed in the enzyme.
 - The cationic intermediates with an sp^3 -hybridized carbon at C2 or C5 (e.g., **5**, **6**, and **7**) are more stable than other possible isomers.
 - According to calculations on **8**, the migration of the azafulvenium moiety in the uroporphyrinogen I σ complex (**5**) should be lower in energy than the migration of an alkyl group and compete well with the migration of hydrogen. Thus, the formation of uroporphyrinogen III (**3**) from hydroxymethylbilane (**2**) by a migration of the acetic and propionic acid side chains in ring D can be excluded.

All the findings are in complete agreement with our proposed mechanism and the results of the biosynthetic investigations for the selective formation of uroporphyrinogen III (**3**) from hydroxymethylbilane (**2**). Thus, in the first step the uroporphyrinogen I σ complex **5** (or its enantiomer) is formed, which is kinetically stabilized, owing to the lack of a base in the enzyme pocket suitably oriented to abstract a proton to give uroporphyrinogen I (**4**). A rearrangement can therefore take place to give the spiro σ complex **6**; in the absence of the enzyme **6** would not be formed, since it is of much higher energy than **5**, according to calculations.^[4] An equilibrium is established between **6**, **5**, and the uroporphyrinogen III σ complex **7**. The latter is then selectively and irreversibly transformed into uroporphyrinogen III (**3**) by abstraction of a proton, presumably through the anion of the acid that is responsible for the elimination of water from hydroxymethylbilane (**2**) to give the azafulvenium ion at the beginning of the biosynthetic cascade. After a long-standing discussion, the proposed mechanism allows, for the first time, an unambiguous explanation for the selective formation of uroporphyrinogen III (**3**) from hydroxymethylbilane (**2**) through the action of cosynthetase.

The calculations on the shift of methyl cations in the pyrrole system clearly show that this follows a suprafacial [1,5]-sigmatropic rearrangement. This nicely explains the high stereoselectivity of one of the steps in the biosynthesis of vitamin B₁₂, namely, the migration of a methyl group from C11 in precorrin_{8x} to C12 in hydrogenobyric acid. This is one of the few examples of a pericyclic reaction in a biosynthetic pathway.

Acknowledgement: Generous financial support by the Deutsche Forschungsgemeinschaft and the Fonds der Chemischen Industrie is gratefully appreciated.

Received: August 5, 1996 [F433]
Revised version: December 5, 1996

- [1] For a recent comprehensive overview see: *Biosynthesis of the Tetrapyrrole Pigments* (Series: Ciba Foundation Symposia) (Eds.: D. J. Chadwick, K. Ackrill), **1994**, 180.
- [2] A. R. Battersby, C. J. R. Fookes, K. E. Gustafson-Potter, E. McDonald, G. W. J. Matcham, *J. Chem. Soc. Perkin Trans. 1* **1982**, 2427–2444.
- [3] a) L. Bogorad, *J. Biol. Chem.* **1958**, *233*, 501–509. b) L. Bogorad, *ibid.* **1958**, *233*, 510–515.
- [4] L. F. Tietze, H. Geißler, *Angew. Chem.* **1993**, *105*, 1087–1089; *Angew. Chem. Int. Ed. Engl.* **1993**, *32*, 1038–1040.
- [5] a) L. F. Tietze, H. Geißler, *Angew. Chem.* **1993**, *105*, 1090–1091; *Angew. Chem. Int. Ed. Engl.* **1993**, *32*, 1040–1042. b) L. F. Tietze, H. Geißler, G. Schulz, *Pure Appl. Chem.* **1994**, *66*, 2303–2306.
- [6] GAUSSIAN 92, M. J. Frisch, G. W. Trucks, M. Head-Gordon, P. M. W. Gill, M. W. Wong, J. B. Foresman, B. G. Johnson, H. B. Schlegel, M. A. Robb, E. S. Replogle, R. Gomperts, J. L. Andres, K. Raghavachari, J. S. Binkley, C. Gonzalez, R. L. Martin, D. J. Fox, D. J. Defrees, J. Baker, J. J. P. Stewart, and J. A. Pople, Gaussian, Inc., Pittsburgh PA, **1992**.
- [7] W. J. Hehre, L. Radom, P. von R. Schleyer, J. A. Pople, *Ab Initio Molecular Orbital Theory*, Wiley, New York, **1985**.
- [8] J. L. Brooker, R. W. Hoffmann, K. N. Houk, *J. Am. Chem. Soc.* **1991**, *113*, 5006–5017.
- [9] This basis set is known to give relative energies that are in good agreement with experimental data: see K. B. Wiberg, E. Martin, *J. Am. Chem. Soc.* **1985**, *107*, 5035–5041.
- [10] VAMP (T. Clark, Universität Erlangen-Nürnberg) is a vectorized version of AMPAC and MOPAC.
- [11] Quantum Chemistry Program Exchange (QCPE) Bloomington, IN 47405, QCPE-No. 455.
- [12] M. J. S. Dewar, E. G. Zoebisch, E. F. Healy, J. J. P. Stewart, *J. Am. Chem. Soc.* **1985**, *107*, 3902–3909.
- [13] J. J. P. Stewart, *J. Comput. Chem.* **1989**, *10*, 209–220, 221–264.
- [14] G. Schulz, *Experimentelle und theoretische Untersuchungen pericyclischer Reaktionen und Ab initio-Berechnung des 1,3-Allylstrain*, Cuvillier, Göttingen, **1995**.
- [15] M. J. D. Powell, J. Chandrasekar, P. H. M. Budzelaar, T. Clark, unpublished results.
- [16] K. N. Houk, Y. Li, J. D. Evanseck *Angew. Chem.* **1992**, *104*, 711–739; *Angew. Chem. Int. Ed. Engl.* **1992**, *31*, 682–728.
- [17] To avoid confusion with the numbering of the unsubstituted heterocycles, the nonsubstituted carbon in **8–10** were numbered as C2.
- [18] a) N. Jux, *GIT Fachz. Lab.* **1991**, *35*, 567–572. b) J. L. Sessler, M. Cyr, A. K. Burrell *Tetrahedron* **1992**, *48*, 9661–9672. c) J. L. Sessler, A. K. Burrell, *Top. Curr. Chem.* **1991**, *161*, 177–271, 272–273.
- [19] a) C. A. Roessner, J. B. Spencer, N. J. Stolowich, J. Wang, G. P. Nayar, P. J. Santander, C. Pichon, C. Min, M. T. Holderman, A. I. Scott, *Chem. Biol.* **1994**, *1*, 119–124. b) A. I. Scott, *Angew. Chem.* **1993**, *105*, 1281–1302; *Angew. Chem. Int. Ed. Engl.* **1993**, *32*, 1223–1243. c) F. Blanche, B. Cameron, J. Crouzet, L. Debussche, D. Thibaut, M. Vuilhorgne, F. J. Leeper, A. R. Battersby, *Angew. Chem.* **1995**, *107*, 421–452; *Angew. Chem. Int. Ed. Engl.* **1995**, *34*, 383–411.
- [20] A. Gossauer, *Die Chemie der Pyrrole*, Springer, Heidelberg, **1974**, p. 131.
- [21] T. Clark, *Handbook of Computational Chemistry*, John Wiley, New York, **1985**.
- [22] a) R. W. Hoffmann, *Chem. Rev.* **1989**, *89*, 1841–1860. b) R. W. Hoffmann, *Angew. Chem.* **1992**, *104*, 1147–1157; *Angew. Chem. Int. Ed. Engl.* **1992**, *31*, 1124–1134.
- [23] L. F. Tietze, G. Schulz, *Liebigs Ann.* **1996**, 1575.
- [24] The energies are not exactly identical in Figure 4 for both minima owing to different conformations of the methyl groups.